4D modeling of the kinematics of a selected subsystem of the Milky Way

I. I. Nikiforov

nii@astro.spbu.ru

Saint Petersburg State University

AMCM 2024:
3rd International Conference on Analytical Methods of Celestial Mechanics

Euler International Mathematical Institute, St. Petersburg, RUSSIA
August 20, 2024

Spatial-kinematic modeling. I

Spatial-kinematic modeling of our Galaxy, the Milky Way, is an analysis of kinematics that allows the kinematic parameters of the centroid of Galactic objects or diffuse matter to depend on the spatial position of the centroid.

Spatial-kinematic modeling. II

Composition of the kinematic model:

- the residual motion of the Sun ($\mathbf{V}_\odot$);
- the differential rotation of the Galaxy, which means that $\omega(R) \neq$ const is a decreasing function, where ω is the angular velocity of rotation, R is the Galactoaxial distance;
- the (natural) dispersion of the velocities of objects relative to the (average) kinematic model;

- the effect of the spiral structure;
- the effect of a non-axisymmetric bar;
- and others.

In this work, we limit ourselves to the first three, basic effects. For other components of the model, either there is no analytical model (bar), or its realism has not been proven (the effect of the spiral structure). But there are enough problems with the first three components, and it is better to start exploring more subtle effects after these problems are mostly solved.

Spatial-kinematic modeling. III

Problems of spatial-kinematic modeling:

- the problem of choosing the general view of the rotation (kinematic) model of the Galaxy;
- statistically justified exclusion of outliers in the data;
- correct algorithm for using the proper motions of reference objects (objects of the selected subsystem);
- separation of measuring and natural velocity dispersions; determination of velocity ellipsoid parameters;
- accounting for the uncertainty of reference distances.

Spatial-kinematic modeling. IV

In addition to the research issues, spatial-kinematic modeling makes it possible to directly determine a number of fundamental characteristics:

- the distance from the Sun to the center of the Galaxy R_0;
- the rotation curve $\theta(R)$, where θ is the linear velocity of rotation;
- the angular and linear velocities of rotation on the solar circle $\theta_0 \equiv \theta(R_0)$ and $\omega_0 \equiv \omega(R_0)$, respectively;
- parameters of the residual motion of the Sun, $(u_\odot, v_\odot, w_\odot) = \mathbf{V}_\odot$;
- the angular and linear velocities of the Sun's rotation around the center of the Galaxy, $\theta_\odot$ and $\omega_\odot$, respectively;
- other derived characteristics.

Spatial-kinematic modeling. V

The Galaxy is a complex system of nested components and subsystems.

Components (in the first approximation):
disk, halo, central component (bar/bulge).

Subsystems are distinguished according to the astrophysical nature of objects/matter, which...

- determines the very possibility of obtaining for each object the observational data necessary for conducting spatial and kinematic modeling —
  - coordinates, i.e., Galactic longitude l and latitude b;
  - velocity characteristics, i.e., heliocentric velocity V_r, proper motion in longitude μ_l and latitude μ_b (directly μ_α, μ_δ);
  - heliocentric distance r;
- gives reason to expect that the selected subsystem is homogeneous in terms of spatial and kinematic properties.

Spatial-kinematic modeling. VI

Subsystems, even belonging to the same component, differ in spatial distribution, origin, age, metallicity and, consequently, kinematics, therefore it is meaningful to model the kinematics of a homogeneous subsystem or take into account the heterogeneity of the sample. Otherwise, we will get «the average temperature in the hospital», which does not represent any of the subsystems.

Only R_0, $\theta_\odot$, and $\omega_\odot$ can be considered universal characteristics.

When developing a new method, the simplest option is a homogeneous subsystem, so we start with it.

Model in general form. I

Definitions.

The model velocity of a given object is called the velocity of the centroid of objects of this type, calculated for the position of this object.

The Subsystem Standard of Rest (SSR), generally not local, is a heliocentric reference frame that moves around the center of the Galaxy in a circle with a velocity equal to the average azimuthal velocity of the objects of the subsystem currently located in the region of the solar ring (in the vicinity of the solar circle $R = R_0$).

The Local Standard of Rest (LSR) is the standard of the circular orbit in the axisymmetric (or azimuthally smoothed) potential of the Galaxy, determined by objects in the small vicinity of the Sun.

Model in general form. II

Assuming a cylindrical model of rotation of centroids of objects around the center of the Galaxy, the model values of the velocity components of the object with coordinates l, b and r are as follows.

$$\begin{aligned} V_{r,\mathsf{mod}} &= V_{r,\mathsf{rot}} + V_{r,\odot}\,, \\ V_{r,\mathsf{rot}} &= [\omega(R) - \omega_0] R_0 \sin l \cos b, \\ V_{r,\odot} &= -u_\odot \cos l \cos b - v_\odot \sin l \cos b - w_\odot \sin b; \end{aligned} \tag{1}$$

$$\begin{aligned} k\mu'_{l,\mathsf{mod}} &= k\mu'_{l,\mathsf{rot}} + k\mu'_{l,\odot}\,, \\ k\mu'_{l,\mathsf{rot}} &= [\omega(R) - \omega_0] \left(\frac{R_0 \cos l}{r} - \cos b \right) - \omega_0 \cos b, \\ k\mu'_{l,\odot} &= (u_\odot \sin l - v_\odot \cos l)/r; \end{aligned} \tag{2}$$

$$\begin{aligned} k\mu_{b,\mathsf{mod}} &= k\mu_{b,\mathsf{rot}} + k\mu_{b,\odot}\,, \\ k\mu_{b,\mathsf{rot}} &= -[\omega(R) - \omega_0] \frac{R_0}{r} \sin l \sin b, \\ k\mu_{b,\odot} &= (u_\odot \cos l \sin b + v_\odot \sin l \sin b - w_\odot \cos b)/r; \end{aligned} \tag{3}$$

Model in general form. III

$$\mu_l' \equiv \frac{dl}{dt}\cos b = \mu_l \cos b, \quad \mu_l \equiv \frac{dl}{dt}; \qquad \mu_b \equiv \frac{db}{dt};$$

$k = 4.7406$ is the coefficient of conversion mu [mas/yr] in mu [km/s/kpc] for r [kpc];

$$R(r) = \sqrt{R_0^2 + r^2\cos^2 b - 2R_0 r \cos l \cos b}; \tag{4}$$

$u_\odot$, $v_\odot$, $w_\odot$ are the components of the residual velocity of the Sun, i.e., the components of the Sun's motion relative to the SSR in the directions $(l, b) = (0°, 0°)$, $(l, b) = (90°, 0°)$, and $b = 90°$, respectively.

Conventional fitting: The least squares method. I

1D fitting:

$$\min \sum_{j=1}^{N} \left\{ \frac{[V_{r,j} - V_{r,\mathrm{mod}}]^2}{(\sigma_{V_r})_j^2} \right\}, \tag{5}$$

N is the sample size.

3D fitting:

$$\min \sum_{j=1}^{N} \left\{ \frac{[V_{r,j} - V_{r,\mathrm{mod}}]^2}{(\sigma_{V_r})_j^2} + \frac{[\mu'_{l,j} - \mu'_{l,\mathrm{mod}}]^2}{(\sigma_{\mu'_l})_j^2} + \frac{[\mu_{b,j} - \mu_{b,\mathrm{mod}}]^2}{(\sigma_{\mu_b})_j^2} \right\}. \tag{6}$$

But $V_{r,\mathrm{mod}} = V_{r,\mathrm{mod}}(r)$, $\mu'_{l,\mathrm{mod}} = \mu'_{l,\mathrm{mod}}(r)$, $\mu_{b,\mathrm{mod}} = \mu_{b,\mathrm{mod}}(r)$
$\Longrightarrow$ Optimizations (5) and (6) are tasks with internal noise
$\Longrightarrow$ Systematic bias of the results.

Conventional fitting: The least squares method. II

This problem became especially relevant after the appearance of mass joint determinations of proper motions and trigonometric parallaxes—e.g., catalogs of maser sources (Reid et al. 2019; VERA Collaboration, Hirota et al. 2020), the Gaia catalog (Gaia Collaboration, Vallenari et al. 2023)

Distant characteristic.

- Distance modulus (relative, i.e., photometric, distances): $d = m - M$, r [kpc] $= 10^{0.2d-2}$.
- Trigonometric parallax (absolute distances): r [kpc] $= 1/\varpi$ [mas].

A common problem of spatial-kinematic modeling: reference objects must be distant $\rightarrow$ random errors of reference distances are also large:

$$\sigma_r = \frac{\ln 10}{5}\,\sigma_d\,r, \qquad \sigma_r = \sigma_\varpi\,r^2, \qquad r_{\text{crit}} = \frac{\ln 10}{5}\,\frac{\sigma_d\ [\text{mag}]}{\sigma_\varpi\ [\text{mas}]}. \quad (7)$$

Approximation of the law of rotation $(\omega(R) - \omega_0)$. I

In the case of a planar subsystem, the linear rotation velocity of the centroids $\theta = \omega R$ can be considered a function that depends only on the Galactoaxial distance R: $\theta = \theta(R)$.
Since the rotation curves of the outer galaxies are flat over a large range of radii, we use a model in the form of a Taylor polynomial to represent precisely $\theta(R)$ [and not $\omega(R)$]:

$$\Theta_n(R) = \sum_{i=0}^{n} \frac{\theta_i}{i!} (\Delta R)^i, \quad n \geq 1, \qquad \theta_i \equiv \left. \frac{d^i \theta}{dR^i} \right|_{R=R_0}, \tag{8}$$

$$\Delta R \equiv R - R_0.$$

$$(\omega - \omega_0) = \left(\frac{\theta}{R} - \omega_0 \right) \approx$$

$$\approx \left[\theta_0 + \theta_1 \Delta R + \frac{1}{2} \theta_2 (\Delta R)^2 + \ \ldots \ + \frac{1}{n!} \theta_n (\Delta R)^n - \omega_0 R \right] R^{-1}, \tag{9}$$

Approximation of the law of rotation $(\omega(R) - \omega_0)$. II

$$\theta_0 - \omega_0 R = \omega_0 R_0 - \omega_0 R = -\omega_0 \Delta R,$$

$$(\omega - \omega_0) \approx \left[(\theta_1 - \omega_0)\Delta R + \sum_{i=2}^{n} \frac{\theta_i}{i!} (\Delta R)^i \right] R^{-1}. \quad (10)$$

Let's introduce the Oort constant:

$$A \equiv -\frac{1}{2} R_0 \omega'(R_0) = -\frac{1}{2} R_0 \left. \frac{d(\theta/R)}{dR} \right|_{R=R_0} = -\frac{1}{2}(\theta_1 - \omega_0). \quad (11)$$

Then

$$(\omega - \omega_0) \approx \left(-2A\Delta R + \sum_{i=2}^{n} \frac{\theta_i}{i!} (\Delta R)^i \right) R^{-1}. \quad (12)$$

$$\theta_1 = -2A + \omega_0. \quad (13)$$

Approximation of the law of rotation $(\omega(R) - \omega_0)$. III

$$T_n(\Delta R) \equiv -2A\Delta R + \sum_{i=2}^{n} \frac{\theta_i}{i!} (\Delta R)^i. \tag{14}$$

$$\begin{aligned} V_{r,\mathsf{rot}} &= T_n(\Delta R)\, \frac{R_0}{R} \sin l \cos b, \\ k\mu'_{l,\mathsf{rot}} &= T_n(\Delta R) \left(\frac{R_0 \cos l}{r} - \cos b \right) R^{-1} - \omega_0 \cos b, \\ k\mu_{b,\mathsf{rot}} &= T_n(\Delta R)\, \frac{R_0}{Rr} \sin l \sin b. \end{aligned} \tag{15}$$

Dispersions of velocity characteristics. I

Natural (dynamic) dispersion of the velocities: the velocity ellipsoid $(\sigma_R, \sigma_\theta, \sigma_Z)$.

$$
\begin{aligned}
(\sigma_{V_r})_j^2 &= (\tilde{\sigma}_{V_r})_j^2 + (\sigma^*_{V_r})_j^2, \\
(\sigma_{\mu'_l})_j^2 &= (\tilde{\sigma}_{\mu'_l})_j^2 + (\sigma^*_{\mu'_l})_j^2, \\
(\sigma_{\mu_b})_j^2 &= (\tilde{\sigma}_{\mu_b})_j^2 + (\sigma^*_{\mu_b})_j^2,
\end{aligned}
\tag{16}
$$

where $\tilde{\sigma}_j^2$ are the measuring variance, $\sigma_j^{*2} = \sigma_j^{*2}(l_j, b_j, r|\sigma_R, \sigma_\theta, \sigma_Z, R_0)$ are contributions of natural dispersion:

$$
\begin{aligned}
\sigma^{*2}_{V_r} &= \sigma_R^2 \cos^2\varphi \cos^2 b + \sigma_\theta^2 \sin^2\varphi \cos^2 b + \sigma_Z^2 \sin^2 b, \\
\sigma^{*2}_{V_l} &= \sigma_R^2 \sin^2\varphi + \sigma_\theta^2 \cos^2\varphi, \\
\sigma^{*2}_{V_b} &= \sigma_R^2 \cos^2\varphi \sin^2 b + \sigma_\theta^2 \sin^2\varphi \sin^2 b + \sigma_Z^2 \cos^2 b.
\end{aligned}
\tag{17}
$$

$$
\sigma^*_{\mu'_l} = \frac{\sigma^*_{V_l}}{kr}, \qquad \sigma^*_{\mu_b} = \frac{\sigma^*_{V_b}}{kr}. \tag{18}
$$

Dispersions of velocity characteristics. II

φ is an angle with a vertex at the point of projection of the object on the Galactic plane between the direction to the center of the Galaxy and the line $l = \text{const}$, $b = 0^\circ$ (between the projections of the major axis of the velocity ellipsoid and the ray of view on the plane of the Galaxy); the angle φ is counted counterclockwise when viewed from the North Pole of the Galaxy:

$$\sin\varphi = \frac{R_0 \sin l}{R(r)}. \tag{19}$$

$$\cos\varphi = \frac{R_0 \cos l - r \cos b}{R(r)}. \tag{20}$$

Conclusion:

A complete solution to the problem, including consideration of all four measurement uncertainties and determination of natural velocity dispersions, is possible only within the framework of the maximum likelihood method.

4D fitting. I

Reid+ (2009) attempted to account for the uncertainty of the parallaxes in the framework of the method of least squares, evaluating model parallax by radial velocity, but then, faced with difficulties $\Longrightarrow$

Reid+ (2014, 2019) abandoned this approach and returned to the usual "velocity-only" fitting. However, the uncertainty of the distance for many masers turns out to be too large to be ignored.

Rastorguev+ (2017,..) take into account the uncertainty of distances within the framework of the maximum likelihood method (MLM) by including partial derivatives of the first order in distance for velocities in the covariance matrix. However, such accounting ignores the non-Gaussian distribution of errors in distances and is suitable only for small uncertainties of the latter.

4D fitting. II

A more perfect idea is the individual reduction of heliocentric distances by including distributions of distant characteristics of objects in the likelihood function.

- Pont+ (1994) applied this approach to photometric distances, using only radial velocities, and while fixing the parameters of the velocity ellipsoid.
- Aghajani & Lindegren (2013); Ding+ (2019): the same approach within the MLM in the case of involving proper motions and parallaxes. However, the analytical solution given by these authors for the reduced (corrected) parallaxes is approximate and can only be applied with small parallax errors.

4D fitting. III

Let the distances r be determined by the trigonometric parallax method: $r = 1/\varpi$, where ϖ — the measured parallax value with the average measurement error σ_ϖ. Then the likelihood function in the case of modeling the 3D velocity field is the product of four probability densities corresponding to the normally distributed random variables V_r, μ'_l, μ_b and ϖ:

$$L = \prod_{j=1}^{N} \frac{1}{\sqrt{2\pi}(\sigma_{V_r})_j} \exp\left\{\frac{[V_{r,j} - V_{r,\mathsf{mod}}(\varpi_{0,j})]^2}{2(\sigma_{V_r})_j^2}\right\} \times$$
$$\times \frac{1}{\sqrt{2\pi}(\sigma_{\mu'_l})_j} \exp\left\{\frac{[\mu'_{l,j} - \mu'_{l,\mathsf{mod}}(\varpi_{0,j})]^2}{2(\sigma_{\mu'_l})_j^2}\right\} \times$$
$$\times \frac{1}{\sqrt{2\pi}(\sigma_{\mu_b})_j} \exp\left\{\frac{[\mu_{b,j} - \mu_{b,\mathsf{mod}}(\varpi_{0,j})]^2}{2(\sigma_{\mu_b})_j^2}\right\} \frac{1}{\sqrt{2\pi}\sigma_{\varpi,j}} \exp\left\{\frac{(\varpi_j - \varpi_{0,j})^2}{2\sigma_{\varpi,j}^2}\right\}, \quad (21)$$

where $V_{r,j}$, $\mu'_{l,j}$, $\mu_{b,j}$ and ϖ_j are the catalog (measured) values of V_r, μ'_l, μ_b and ϖ for the j-th object;

4D fitting. IV

$\varpi_{0,j}$ is the reduced parallax value of the j-th object;
$\Pi_{0,j} \sim \mathrm{N}(\varpi_j, \sigma^2_{\varpi,j})$.
The triple of values $(l_j, b_j, \varpi_{0,j})$ defines the point of the (non-orthogonal) projection of the object onto the kinematic model (rotation curve), taking into account all uncertainties.

$$\mathcal{L} \equiv -\ln L = \mathcal{L}^{(0)} + \mathcal{L}^{(1)}(\mathbf{a}),$$

$$\mathcal{L}^{(0)} = 4N \ln\sqrt{2\pi} + \sum_{j=1}^{N} [\ln \sigma_{\varpi,j}] = \text{const},$$

$$\mathcal{L}^{(1)}(\mathbf{a}) = \sum_{j=1}^{N} \left\{ \ln[\sigma_{V_r}(\varpi_{0,j})]_j + \ln[\sigma_{\mu'_l}(\varpi_{0,j})]_j + \ln[\sigma_{\mu_b}(\varpi_{0,j})]_j \right\} +$$
$$+ \frac{1}{2} \sum_{j=1}^{N} \min_{\varpi_{0,j}} \left\{ \frac{[V_{r,j} - V_{r,\mathsf{mod}}(\varpi_{0,j})]^2}{[\sigma_{V_r}(\varpi_{0,j})]^2_j} + \frac{[\mu'_{l,j} - \mu'_{l,\mathsf{mod}}(\varpi_{0,j})]^2}{[\sigma_{\mu'_l}(\varpi_{0,j})]^2_j} + \right.$$
$$\left. + \frac{[\mu_{b,j} - \mu_{b,\mathsf{mod}}(\varpi_{0,j})]^2}{[\sigma_{\mu_b}(\varpi_{0,j})]^2_j} + \frac{(\varpi_j - \varpi_{0,j})^2}{\sigma^2_{\varpi,j}} \right\}. \quad (22)$$

4D fitting. V

4D fitting:

$$\mathcal{L}^{(1)}(\mathbf{a}) \to \min, \tag{23}$$

$\mathbf{a} = (R_0, \omega_0, A, \theta_2, \ \ldots, \ \theta_n, u_\odot, v_\odot, w_\odot, \sigma_R, \sigma_\theta, \sigma_Z)$ is the vector of model parameters.

Algorithm. I

- Level I. The solution for $n = \text{const}$ and a fixed sample of N objects.
- Level II. Optimization of the order of the model rotation curve (Nikiforov 1999a,b).
  The dependence of the characteristics that reflect the quality of the solution on the order of the model: $\sigma^2(n)$ [$\mathcal{L}^{(1)}(n)$, $\sigma^2_\theta(n)$, etc.]
  We are looking for a set of acceptable orders $\{\widetilde{n}_\mathrm{o}\}$, which includes consecutive values of n according to the rule

$$\sigma^2(n) \approx \mathrm{const} \quad \forall\, n \in \{\widetilde{n}_\mathrm{o}\}. \tag{24}$$

  Then these values of $\widetilde{n}_\mathrm{o}$ are strictly limited from above to the minimum of the orders of n, in which...

Algorithm. II

1) all coefficients of θ_i become insignificant:

$$\sigma_{\theta_i}/\theta_i \gtrsim 0.5 \quad \forall\ 2 \leq i \leq n \tag{25}$$

(special t-criterion for testing the hypothesis $\mathcal{H}_0$: $\theta_i = 0$ for the significance level of 0.05);

2) the significance of the higher coefficient θ_n decreases to the level of 1σ:

$$\sigma_{\theta_n}/\theta_n \gtrsim 1; \tag{26}$$

3) the $\Theta_n(R)$ model turns out to be clearly unrealistic at the edges of the R interval.

After applying all the constraints to the set of acceptable models with orders of $\{\widetilde{n}_\mathrm{o}\}$ (as as a rule, from one to three) fall into the simplest models of the rotation curve possible. If $\{\widetilde{n}_\mathrm{o}\}$ consists of a single element, then this value is taken as optimal, n_o. Then the final results are those that were obtained for $n = n_\mathrm{o}$. If there are more than one valid orders, then some kind of averaging procedure may be needed for some parameters.

Algorithm. III

- Level III. Level III. Exclusion of outliers.
  For results obtained in a fixed acceptable order $\widetilde{n}_o$, objects with redundant residuals are searched and excluded.
  We use a flexible algorithm for excluding objects with large residuals.
  - One-dimensional algorithm (Nikiforov 2012).
    1. For a given sample size N, the value of κ is calculated, which satisfies the equation

$$[1 - \psi(\kappa)]\, N = 1, \tag{27}$$

where $\psi(z)$ is probability integral:

$$\psi(z) = \sqrt{\frac{2}{\pi}} \int_0^z e^{-\frac{1}{2}t^2} dt. \tag{28}$$

Algorithm. IV

2. We determine the number of objects L of this sample that meet the conditions

$$\frac{|\delta_j|}{\sigma_j} > \kappa. \tag{29}$$

The mathematical expectation of this number is equal to one with a normal distribution of residuals. A larger number of such objects may be considered as redundant with one or another probability.

3. If $L > 1$, then $L - L'$ objects with the largest residual modules are excluded from further consideration, where $L' \geq 1$ is a parameter of this algorithm.

4. To the remaining objects, i.e., in particular, when $L = 1$, the following criterion is applied: objects with residuals

$$\frac{|\delta_j|}{\sigma_j} > k_\gamma(N), \tag{30}$$

are excluded, where k_γ is the root of the equation

$$1 - [\psi(k_\gamma)]^N = \gamma, \tag{31}$$

here γ is the accepted significance level. We used $\gamma = 0.05$ (approximately the significance level 2σ).

- Generalization of one-dimensional algorithm to a four-dimensional field of residuals based on statistics χ^2_4.

$$z_j = \frac{[V_{r,j} - V_{r,\mathsf{mod}}(\varpi_{0,j})]^2}{(\sigma_{V_r})^2_j} + \frac{[\mu'_{l,j} - \mu'_{l,\mathsf{mod}}(\varpi_{0,j})]^2}{(\sigma_{\mu'_l})^2_j} + \\ + \frac{[\mu_{b,j} - \mu_{b,\mathsf{mod}}(\varpi_{0,j})]^2}{(\sigma_{\mu_b})^2_j} + \frac{(\varpi_j - \varpi_{0,j})^2}{\sigma^2_{\varpi,j}}. \tag{32}$$

$$[1 - F_4(\kappa)]N = 1, \tag{33}$$

$$1 - F_4(z) = P(\chi^2_4 > z) = e^{-z/2}\left(\frac{z}{2} + 1\right). \tag{34}$$

$$P(L) = \frac{e^{-1}}{L!}. \tag{35}$$

Тогда

$$\begin{aligned} P(L \geq 2) &\cong 0.264, \\ P(L \geq 3) &\cong 0.080, \\ P(L \geq 4) &\cong 0.019. \end{aligned} \tag{36}$$

Based on these values, the number $L = 4$ can be considered clearly redundant, i.e., take $L' = 3$. To obtain unbiased estimates of the non-dispersive parameters of the model, we select $L' = 1$.

Algorithm. VII

A single application of the algorithms of levels I–III is one iteration. If, according to its results, the sample has decreased, in the next iteration there is a new solution to the problem for the remaining sample, i.e., algorithms of levels I and II are executed. Then the algorithms of level III are applied again. The shutdown occurs when exceptions are no longer needed in the next iteration

Data. I

Masers with trigonometric parallaxes.

Since about 2007, a number of groups have been intensively engaged in measuring trigonometric parallaxes and the corresponding movements of maser eruption sources associated with massive star formation regions. Radiation (interferometry with an ultra-long base) of masers is carried out at a methanol frequency (CH_3OH) 12 GHz, H_2O 22 GHz, SiO $\rightarrow$

A new type of reference objects: masers with trigonometric parallaxes to distances of $\sim$10 kpc with 3D velocities.

Application of the kinematic method to masers.

Reid+ (2009): $N = 16$, $R_0 = 8.4 \pm 0.6$ kpc.
Reid+ (2014): $N = 80$ out of 103, $R_0 = 8.34 \pm 0.16$ kpc.
Rastorguev+ (2017): $N = 131$, $R_0 \approx 8.24 \pm 0.12$ kpc.
Reid+ (2019): $N = 147$ from $\approx$200 HMSFR masers, $R_0 = 8.15 \pm 0.15$ kpc.

Data. II

VERA Collaboration et al. (2020): $N = 224$, SFRs and RSG masers from VERA and Reid+ (2019) catalogs,
$R_0 = 7.92 \pm 0.16_{\text{stat.}} \pm 0.3_{\text{sys.}}$ kpc.

This paper.

From maser sources, the HMSFR class masers are of the greatest interest for studying the kinematics of the Galaxy as a very "cold" subsystem of a thin disk with absolute distances, moreover, characterized by small parallax uncertainties even for large heliocentric distances (Nikiforov & Veselova, 2018b). To obtain a sample of HMSFR measurements, we used the catalogues in Reid+ (2019), VERA+ (2020), supplementing them with new data from the literature: Xu+ (2021), Sakai+ (2021), Bian+ (2022), Mai+(2023), Hyland+ (2023), Hyland+ (2024). Total data for 280 masers. The full sample of HMSFRs: $N = 210$.

Data. III

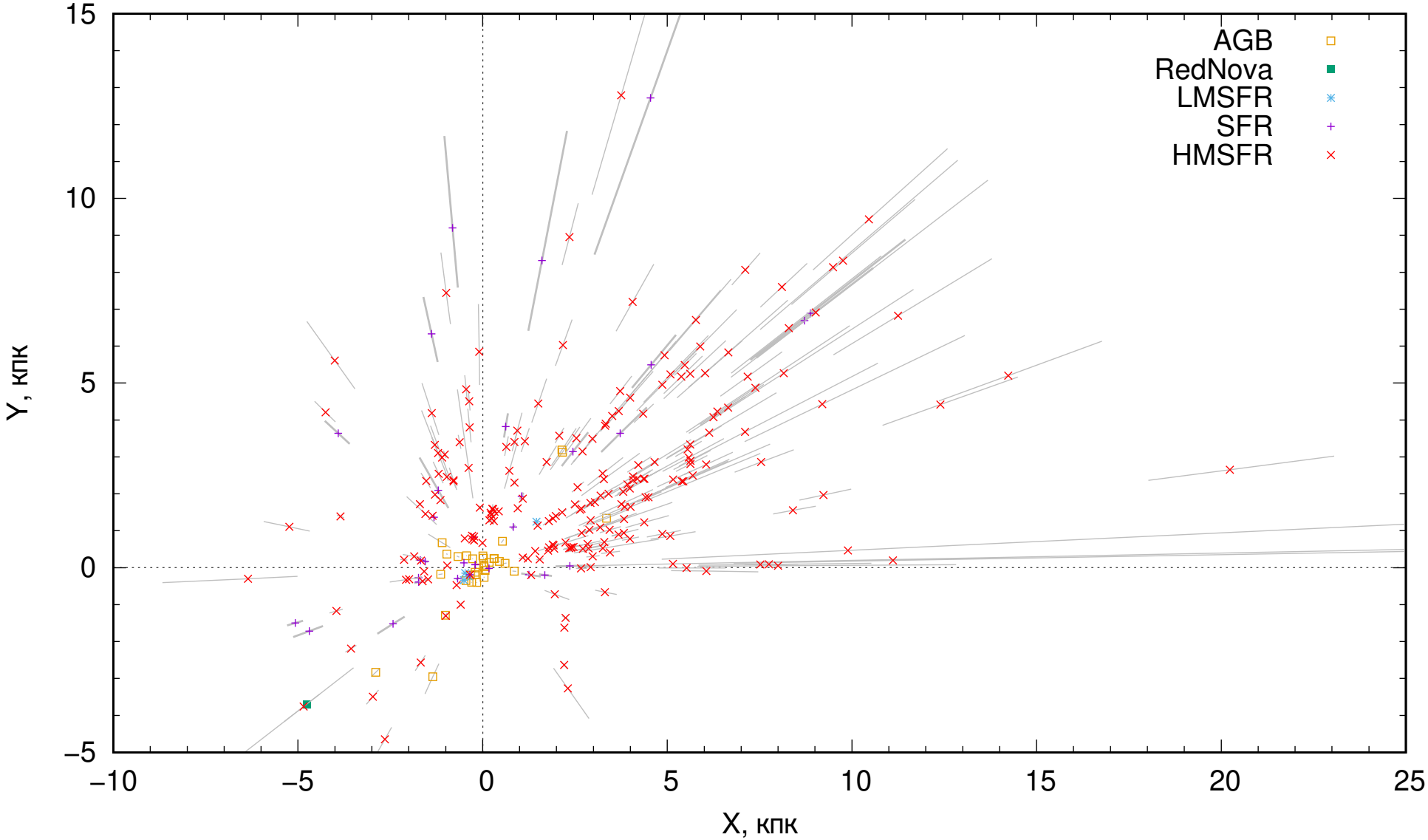
AGB
RedNova
LMSFR
SFR
HMSFR
Y, кпк
X, кпк
15
10
5
0
−5
−10
−5
0
5
10
15
20
25

Data. IV

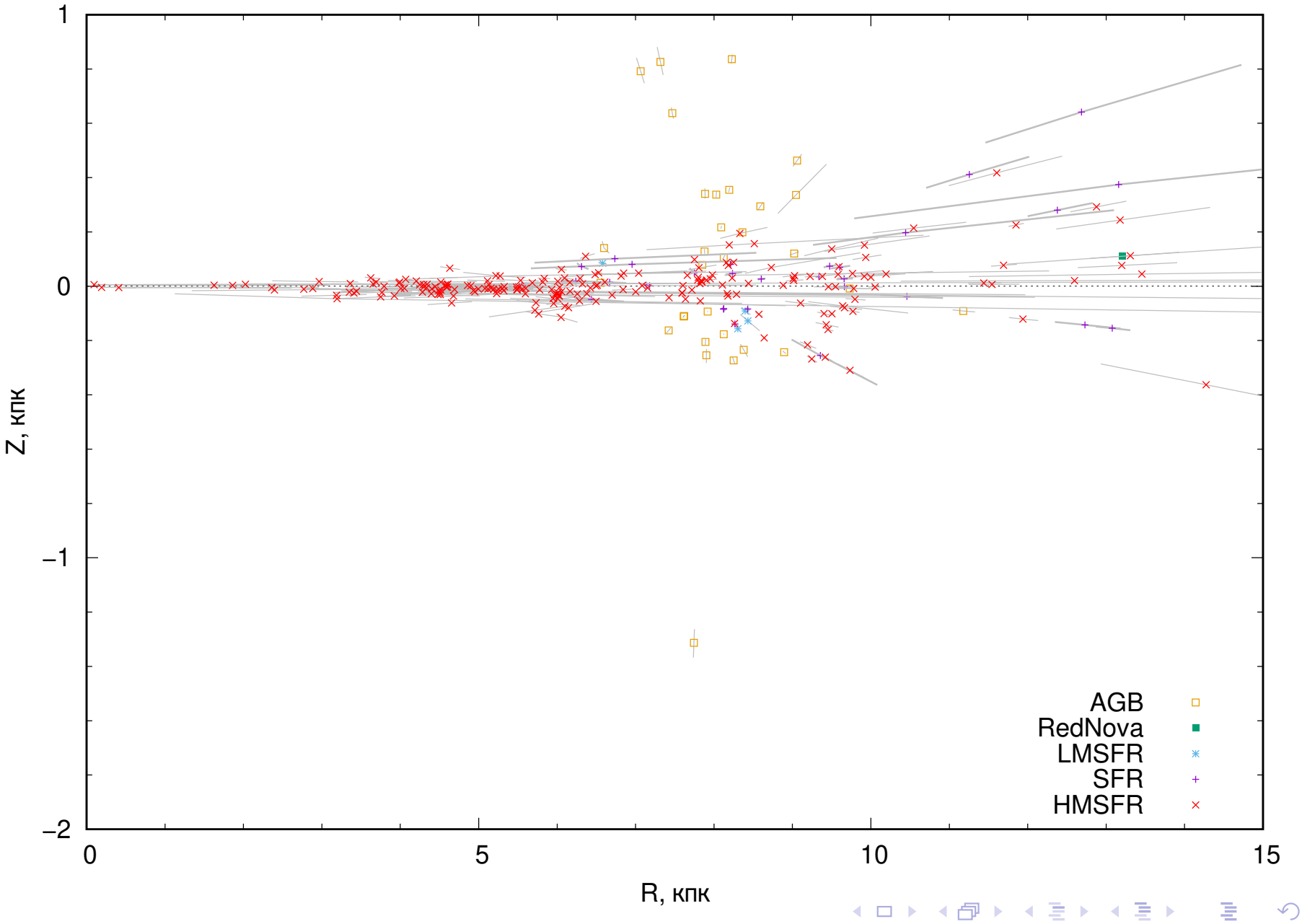

Data. V

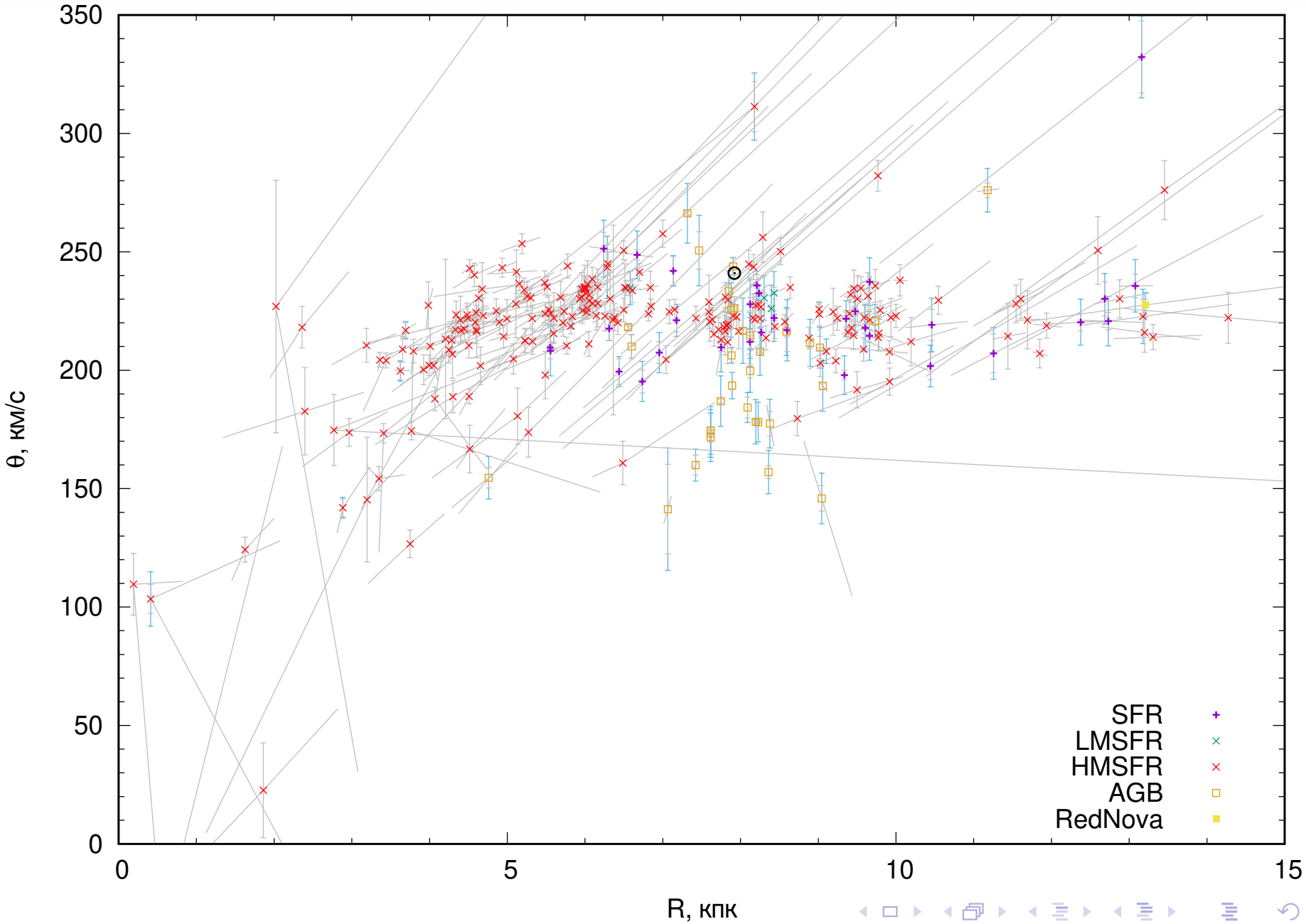
350
300
250
200
150
100
50
0
θ, км/с
0
5
10
15
R, кпк
SFR
LMSFR
HMSFR
AGB
RedNova

Results. I

Final sample. $L' = 3$: $N = 201$, $L' = 1$: $N = 197$;
$n_o = 3$.

n	R_0	ω_0	A	$u_\odot$	$v_\odot$	$w_\odot$	σ_R	σ_θ	σ_Z
1	7.698	27.94	13.83	5.14	18.06	8.12	9.36	6.36	3.45
	$^{+0.121}_{-0.118}$	± 0.24	± 0.19	± 1.00	± 0.90	± 0.52	$^{+0.92}_{-0.79}$	± 0.91	$^{+0.64}_{-0.65}$
2	7.965	28.73	14.34	6.07	13.40	8.23	6.81	6.67	3.48
	$^{+0.128}_{-0.124}$	± 0.23	± 0.20	± 0.88	± 1.01	± 0.52	$^{+0.87}_{-0.79}$	$^{+0.87}_{-0.85}$	$^{+0.65}_{-0.66}$
3	**7.881**	**28.43**	**15.45**	**6.09**	**15.55**	**8.22**	**7.13**	**4.64**	**3.46**
	$^{\mathbf{+0.119}}_{\mathbf{-0.115}}$	$\mathbf{\pm 0.22}$	$\mathbf{\pm 0.23}$	$\mathbf{\pm 0.86}$	$\mathbf{\pm 0.92}$	$\mathbf{\pm 0.52}$	$^{\mathbf{+0.83}}_{\mathbf{-0.77}}$	$^{\mathbf{+0.84}}_{\mathbf{-0.85}}$	$^{\mathbf{+0.64}}_{\mathbf{-0.65}}$
4	7.879	28.43	15.44	6.09	15.58	8.22	7.15	4.60	3.44
	$^{+0.122}_{-0.118}$	± 0.22	$^{+0.33}_{-0.32}$	± 0.86	± 0.96	± 0.52	$^{+0.83}_{-0.77}$	$^{+0.84}_{-0.86}$	$^{+0.64}_{-0.65}$
5	7.885	28.38	15.58	6.06	15.96	8.22	7.18	4.56	3.44
	$^{+0.122}_{-0.118}$	± 0.23	± 0.33	± 0.86	$^{+1.10}_{-1.04}$	± 0.52	$^{+0.83}_{-0.78}$	$^{+0.85}_{-0.86}$	$^{+0.64}_{-0.65}$
6	7.887	28.38	15.99	6.06	15.75	8.22	7.13	4.65	3.45
	$^{+0.123}_{-0.118}$	± 0.23	± 0.46	± 0.86	$^{+1.14}_{-1.16}$	± 0.52	$^{+0.83}_{-0.78}$	$^{+0.86}_{-0.87}$	$^{+0.64}_{-0.65}$
7	7.87	27.92	16.19	5.83	18.57	8.22	7.22	4.21	3.43
	± 0.15	± 0.26	$^{+0.59}_{-0.46}$	$^{+0.85}_{-0.86}$	$^{+1.30}_{-1.31}$	± 0.52	$^{+0.85}_{-0.76}$	$^{+0.85}_{-0.87}$	$^{+0.64}_{-0.66}$

Results. II

n	θ_2	θ_3	θ_4	θ_5	θ_6	θ_7
1						
2	-1.95					
	± 0.22					
3	$\mathbf{-1.34}$	$\mathbf{1.036}$				
	$\mathbf{\pm 0.20}$	$\mathbf{^{+0.145}_{-0.140}}$				
4	-1.31	1.02	-0.014			
	± 0.39	$^{+0.22}_{-0.20}$	$^{+0.166}_{-0.158}$			
5	-0.96	1.40	-0.182	-0.191		
	$^{+0.51}_{-0.45}$	$^{+0.44}_{-0.41}$	$^{+0.172}_{-0.191}$	$^{+0.170}_{-0.183}$		
6	-1.41	2.48	0.70	-0.90	-0.70	
	$^{+0.82}_{-0.85}$	± 0.92	$^{+0.82}_{-0.80}$	$^{+0.65}_{-0.63}$	$^{+0.61}_{-0.58}$	
7	3.70	5.5	-6.36	-6.97	4.93	6.0
	$^{+1.62}_{-1.16}$	± 1.2	± 2.1	$^{+1.58}_{-3.16}$	$^{+1.70}_{-1.06}$	$^{+3.1}_{-1.0}$

Results. III

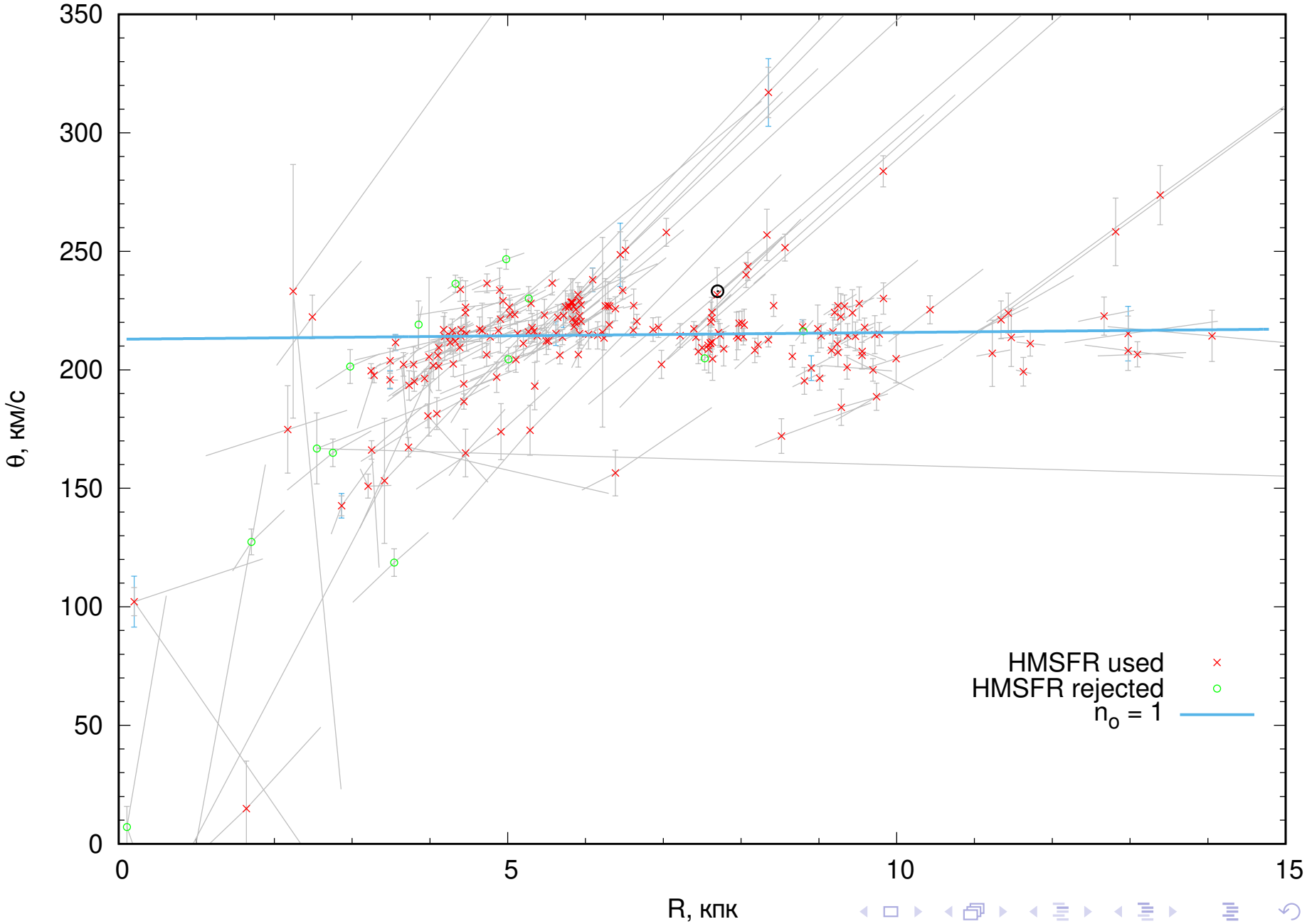
350
300
250
200
150
100
50
0
θ, км/с
0
5
10
15
R, кпк
HMSFR used
HMSFR rejected
$n_o = 1$

Results. IV

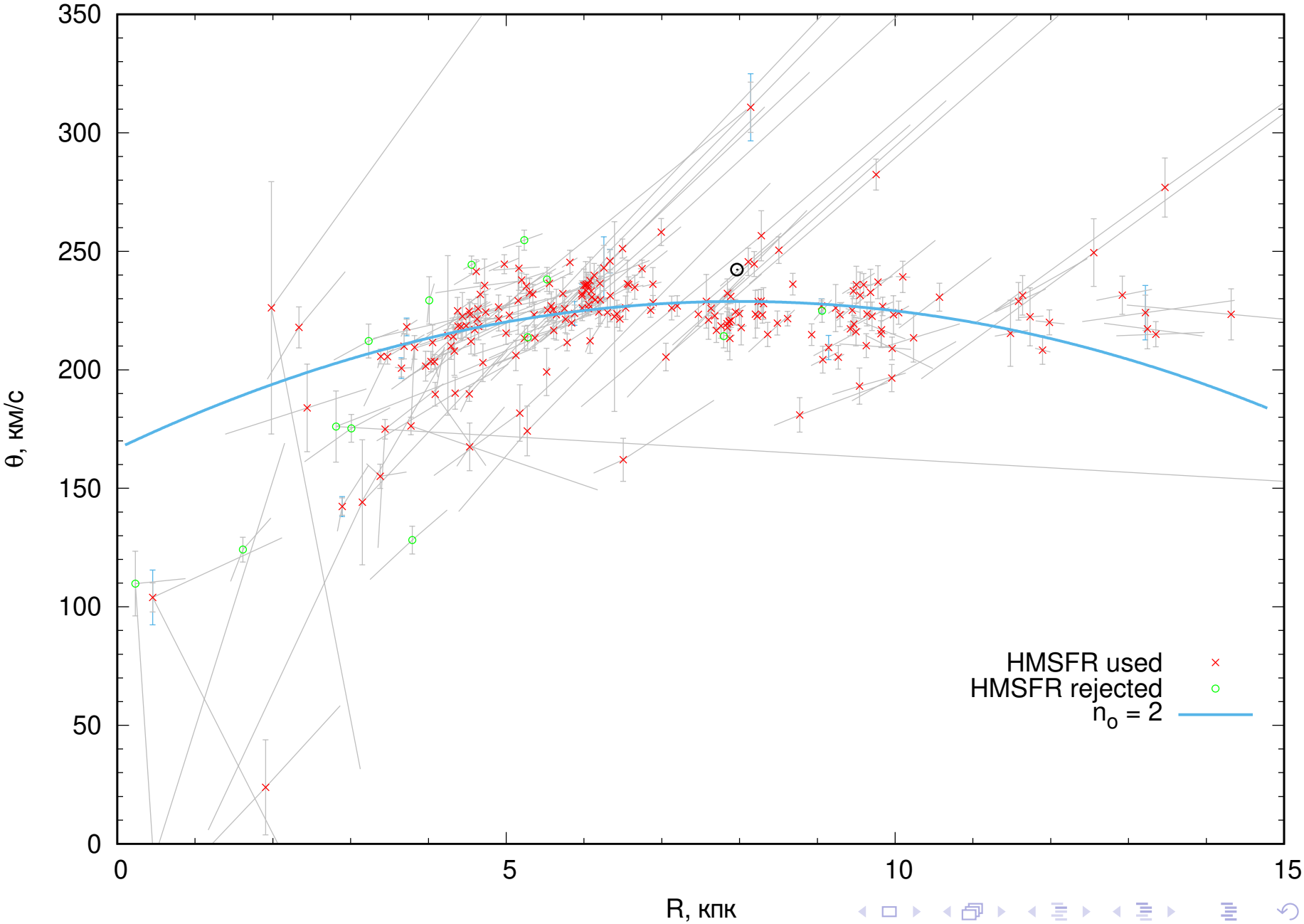
350
300
250
200
150
100
50
0
θ, км/с
0
5
10
15
R, кпк
HMSFR used
HMSFR rejected
$n_o = 2$

Results. V

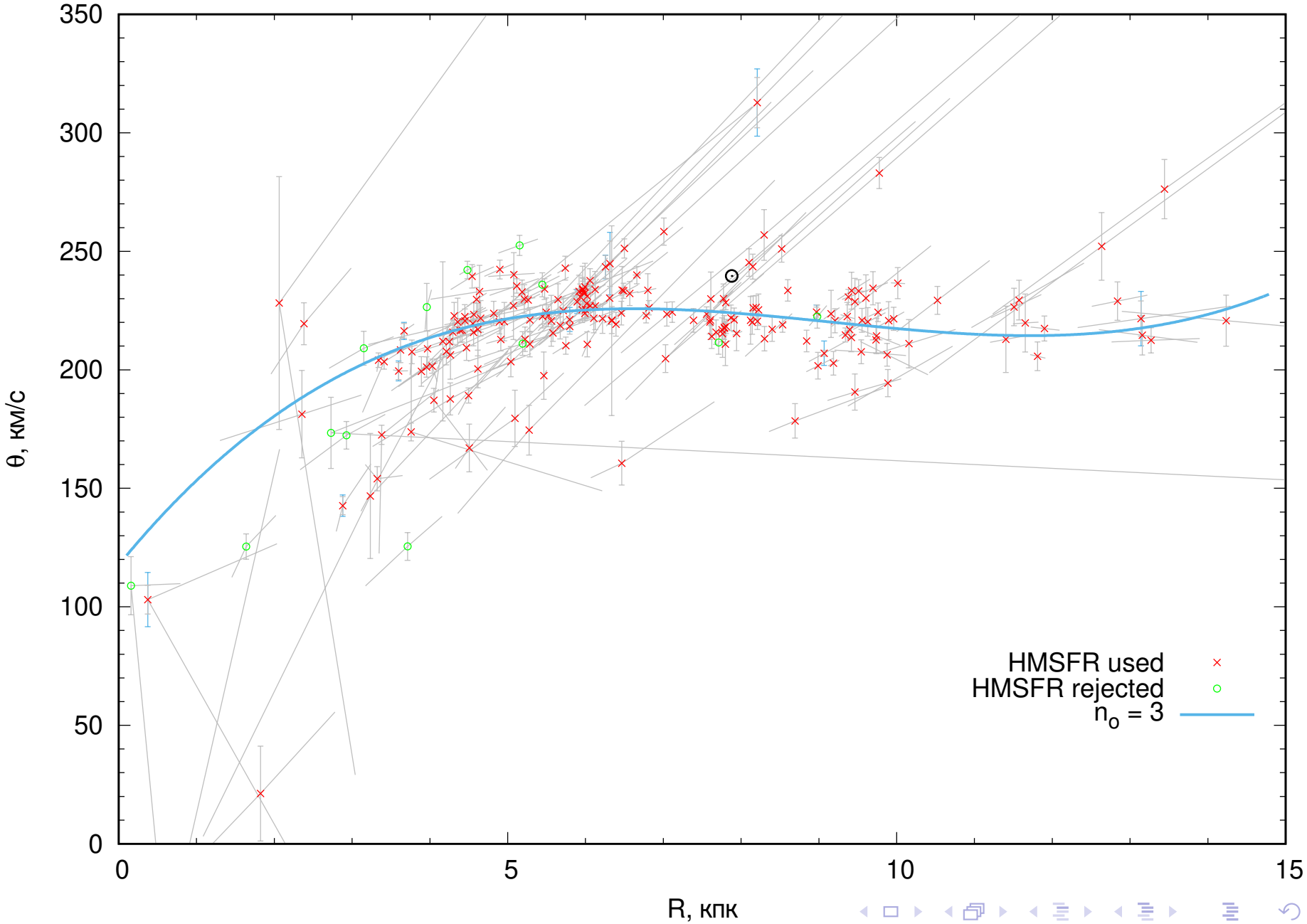
350
300
250
200
150
100
50
0
θ, км/с
0
5
10
15
R, кпк
HMSFR used
HMSFR rejected
$n_o = 3$

Results. VI

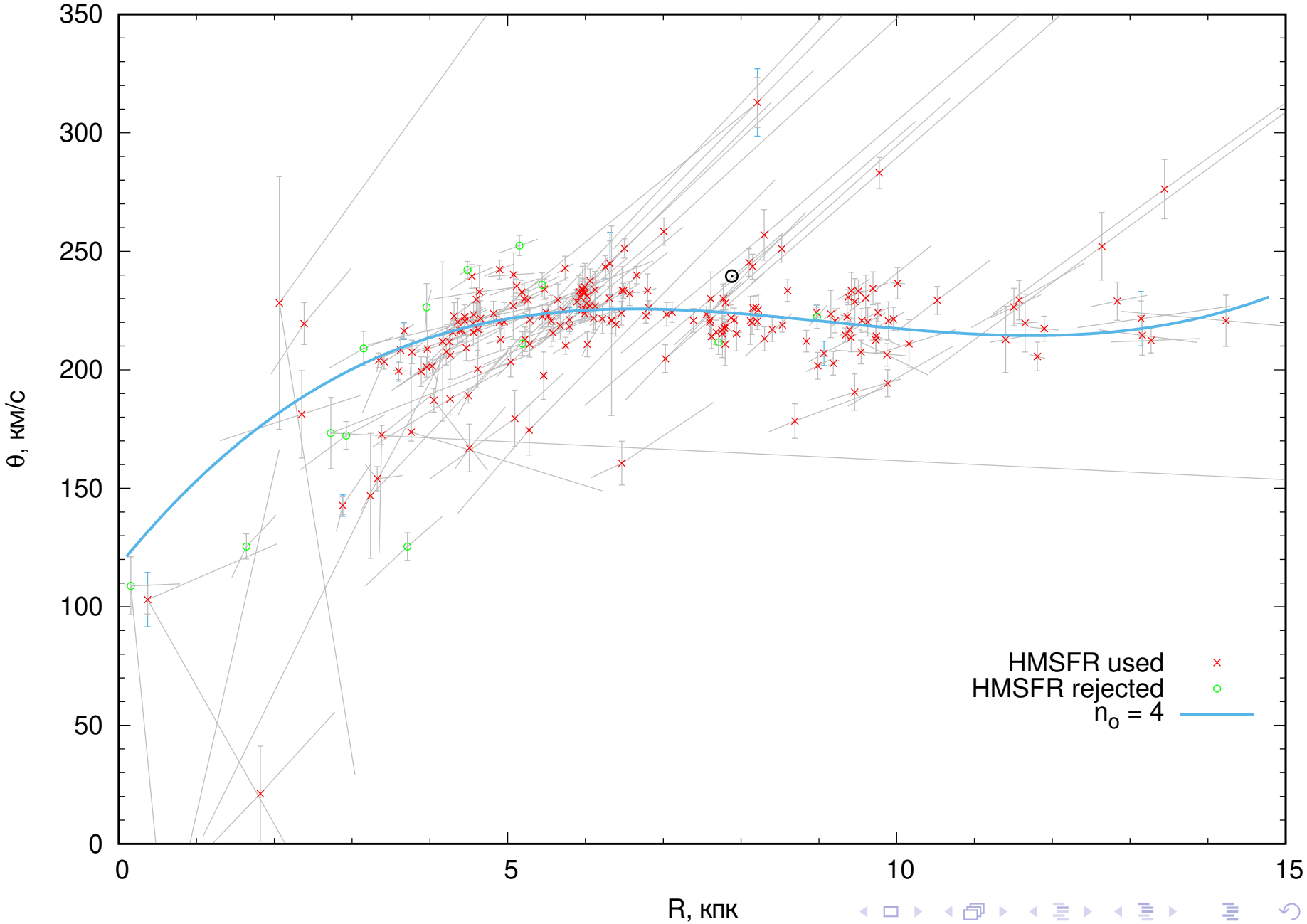
350
300
250
200
150
100
50
0
θ, км/с
0
5
10
15
R, кпк
HMSFR used
HMSFR rejected
$n_o = 4$

Results. VII

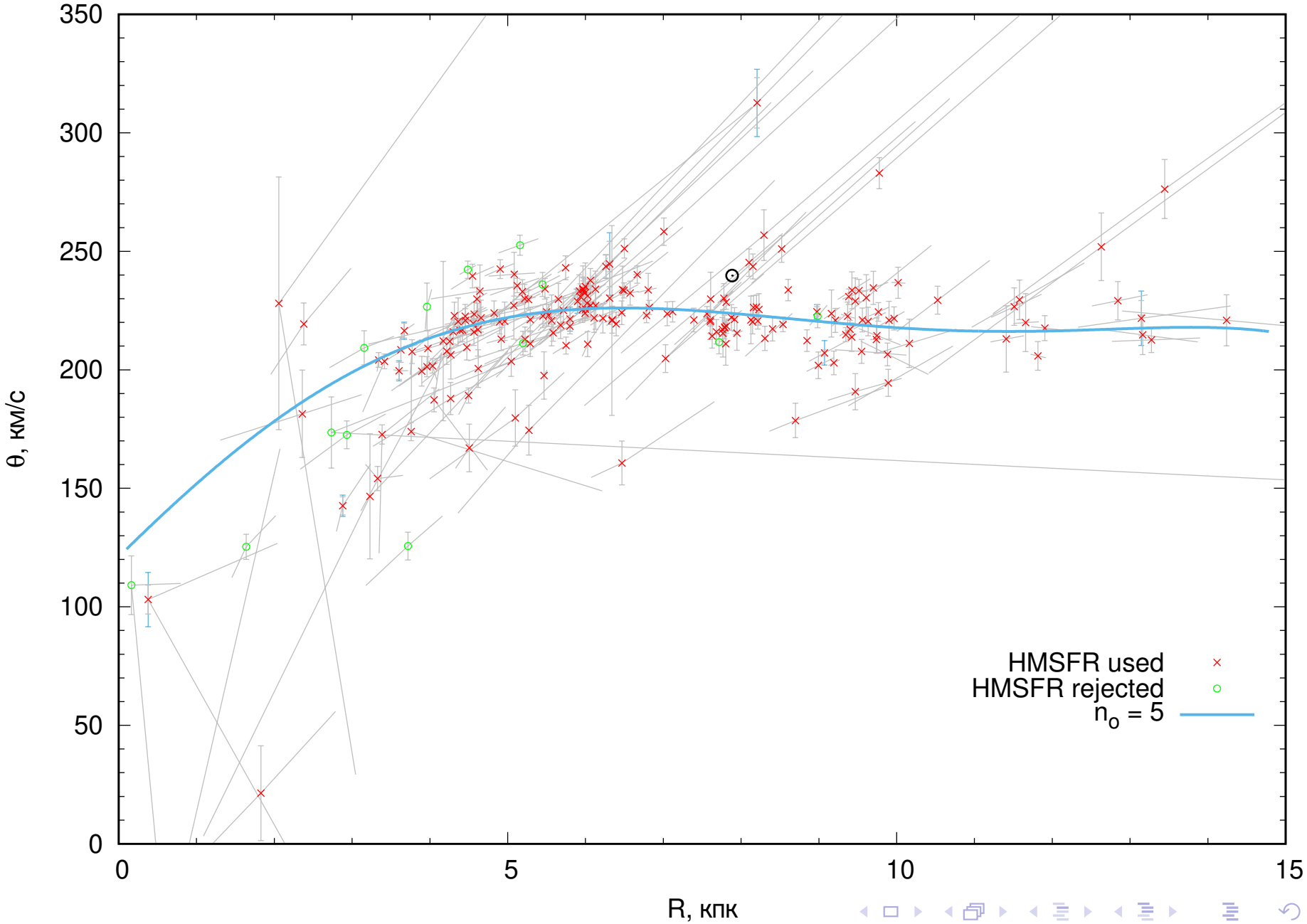
350
300
250
200
150
100
50
0
θ, км/с
0
5
10
15
R, кпк
HMSFR used
HMSFR rejected
$n_o = 5$

Results. VIII

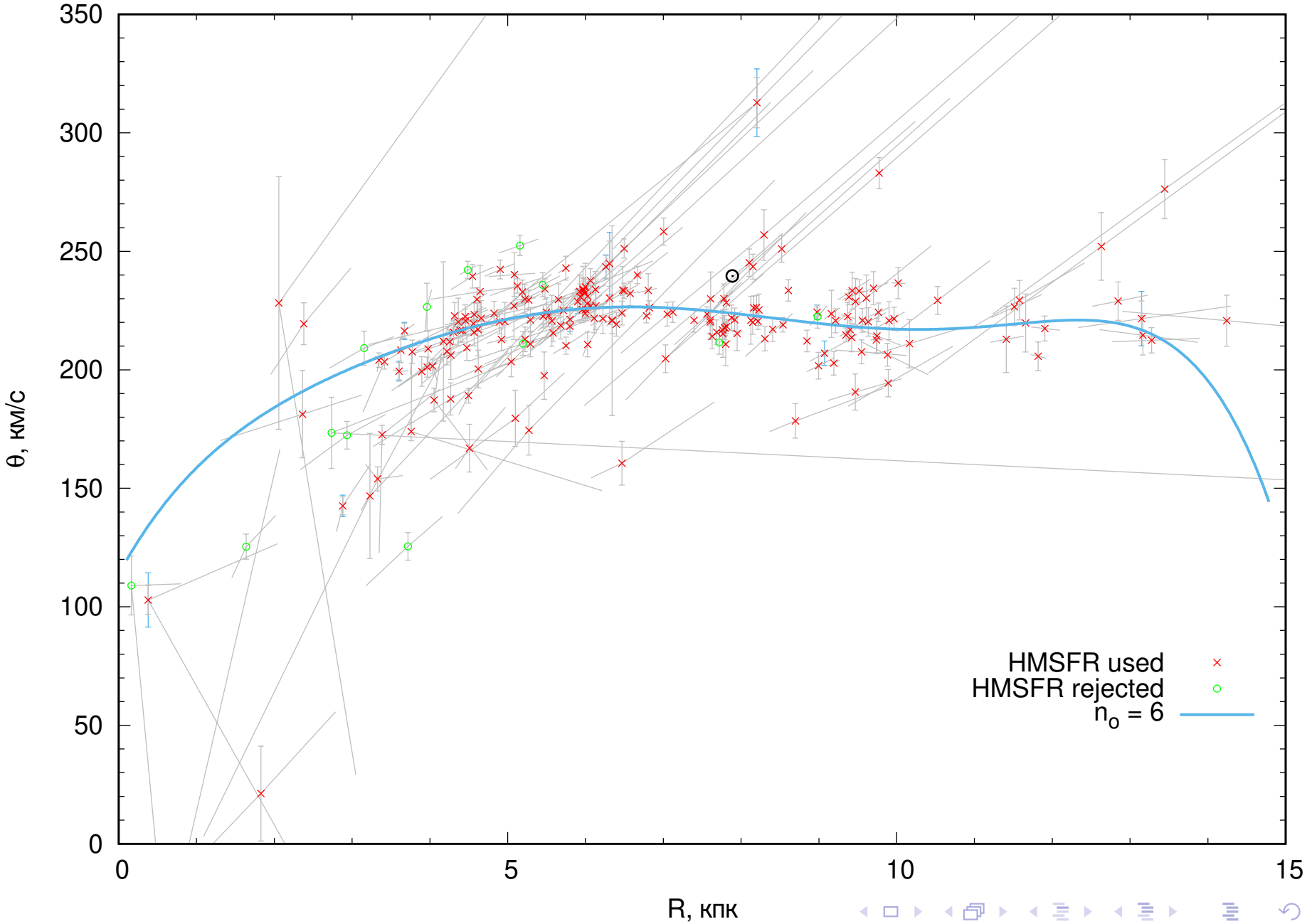

Results. IX

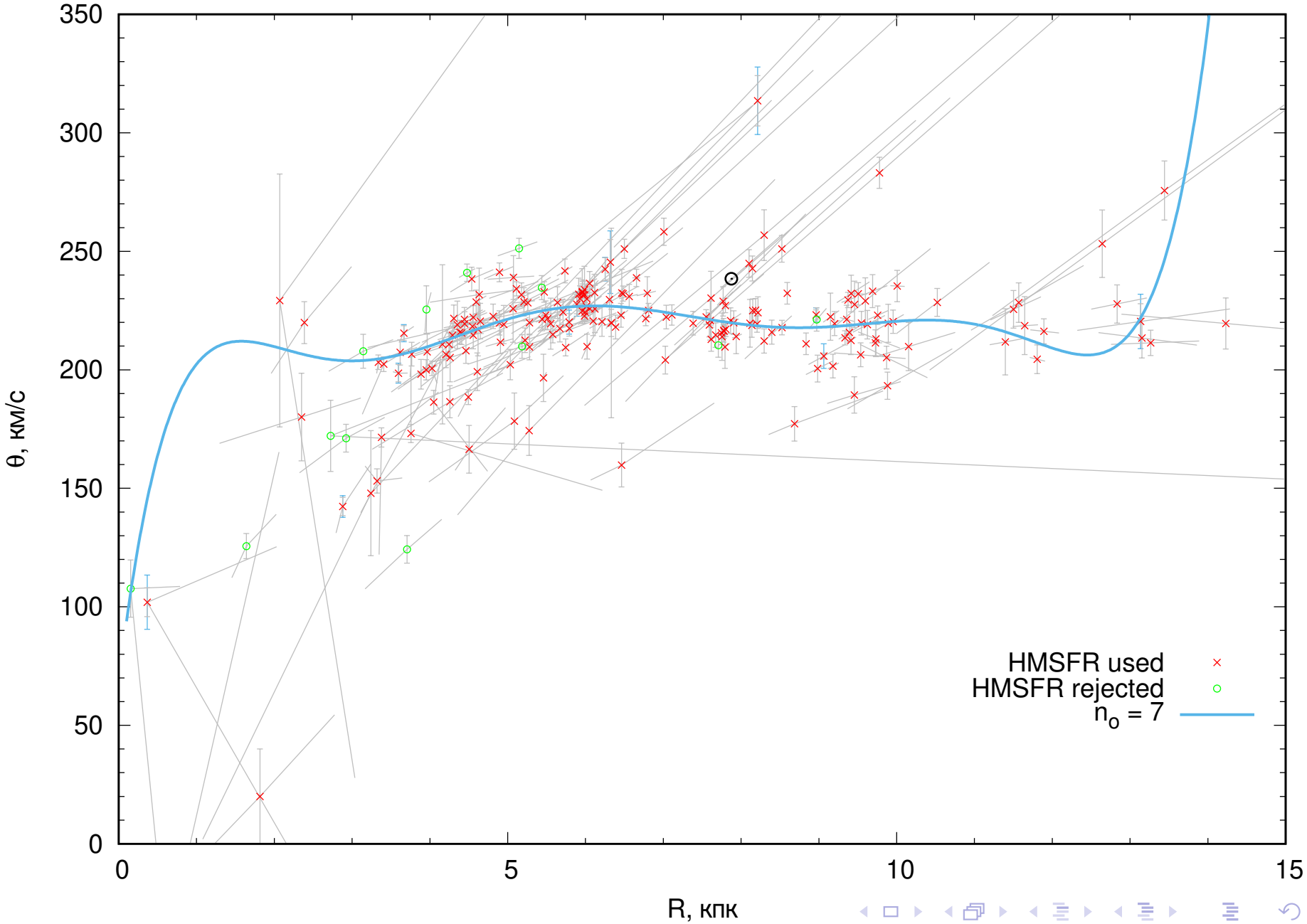
350
300
250
200
150
100
50
0
θ, км/с
0
5
10
15
R, кпк
HMSFR used
HMSFR rejected
$n_o = 7$

Results. X

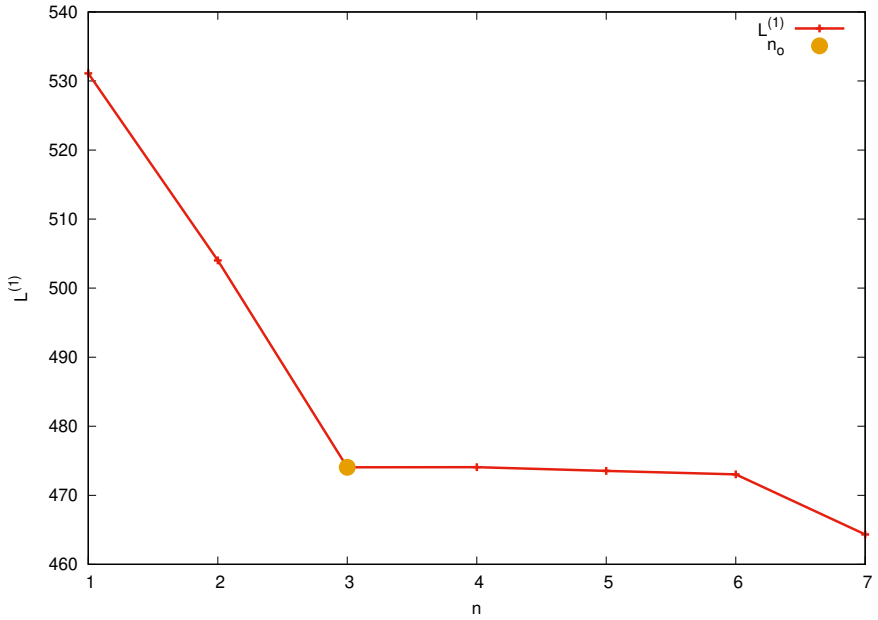

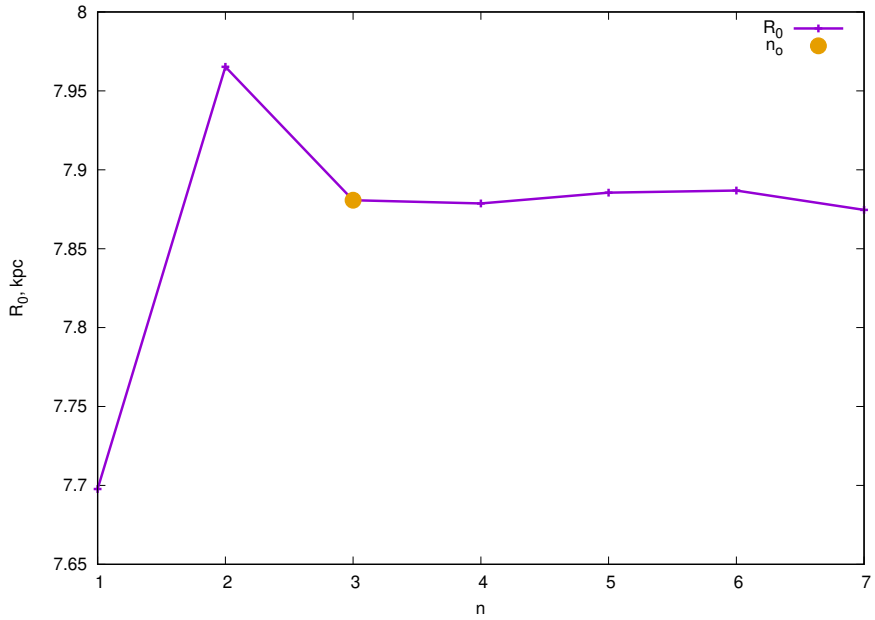

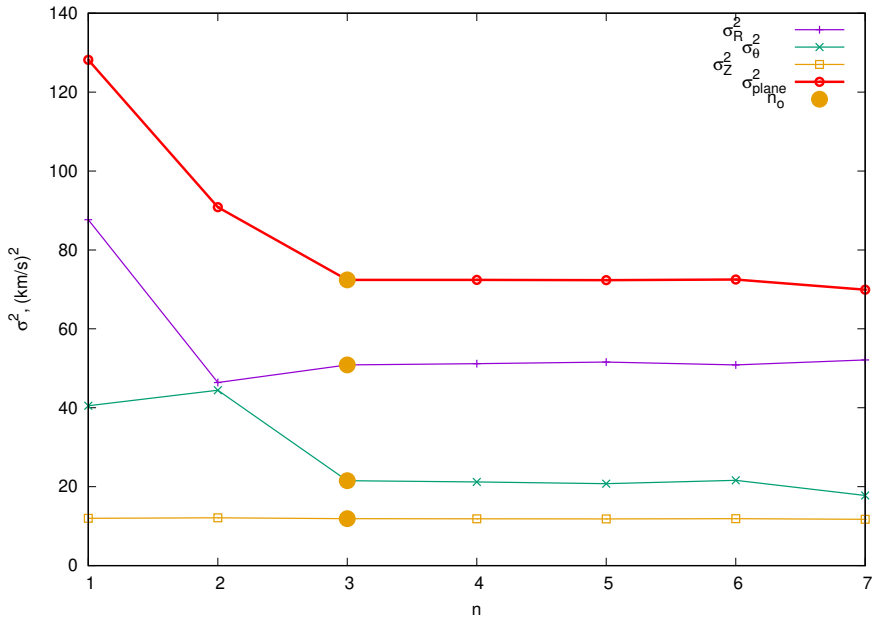

$$\sigma^2_{\text{plane}} \equiv \sigma^2_R + \sigma^2_\theta.$$

Results. XI

n	R_0	ω_0	A	$u_\odot$	$v_\odot$	$w_\odot$	σ_R	σ_θ	σ_Z
1	7.698	27.94	13.83	5.14	18.06	8.12	9.36	6.36	3.45
	$^{+0.121}_{-0.118}$	±0.24	±0.19	±1.00	±0.90	±0.52	$^{+0.92}_{-0.79}$	±0.91	$^{+0.64}_{-0.65}$
2	7.965	28.73	14.34	6.07	13.40	8.23	6.81	6.67	3.48
	$^{+0.128}_{-0.124}$	±0.23	±0.20	±0.88	±1.01	±0.52	$^{+0.87}_{-0.79}$	$^{+0.87}_{-0.85}$	$^{+0.65}_{-0.66}$
3	**7.881**	**28.43**	**15.45**	**6.09**	**15.55**	**8.22**	**7.13**	**4.64**	**3.46**
	$^{\mathbf{+0.119}}_{\mathbf{-0.115}}$	$\mathbf{\pm0.22}$	$\mathbf{\pm0.23}$	$\mathbf{\pm0.86}$	$\mathbf{\pm0.92}$	$\mathbf{\pm0.52}$	$^{\mathbf{+0.83}}_{\mathbf{-0.77}}$	$^{\mathbf{+0.84}}_{\mathbf{-0.85}}$	$^{\mathbf{+0.64}}_{\mathbf{-0.65}}$
4	7.879	28.43	15.44	6.09	15.58	8.22	7.15	4.60	3.44
	$^{+0.122}_{-0.118}$	±0.22	$^{+0.33}_{-0.32}$	±0.86	±0.96	±0.52	$^{+0.83}_{-0.77}$	$^{+0.84}_{-0.86}$	$^{+0.64}_{-0.65}$
5	7.885	28.38	15.58	6.06	15.96	8.22	7.18	4.56	3.44
	$^{+0.122}_{-0.118}$	±0.23	±0.33	±0.86	$^{+1.10}_{-1.04}$	±0.52	$^{+0.83}_{-0.78}$	$^{+0.85}_{-0.86}$	$^{+0.64}_{-0.65}$
6	7.887	28.38	15.99	6.06	15.75	8.22	7.13	4.65	3.45
	$^{+0.123}_{-0.118}$	±0.23	±0.46	±0.86	$^{+1.14}_{-1.16}$	±0.52	$^{+0.83}_{-0.78}$	$^{+0.86}_{-0.87}$	$^{+0.64}_{-0.65}$
7	7.87	27.92	16.19	5.83	18.57	8.22	7.22	4.21	3.43
	±0.15	±0.26	$^{+0.59}_{-0.46}$	$^{+0.85}_{-0.86}$	$^{+1.30}_{-1.31}$	±0.52	$^{+0.85}_{-0.76}$	$^{+0.85}_{-0.87}$	$^{+0.64}_{-0.66}$

Results. XII

n	θ_0	θ_1	$\theta_\odot$	$\omega_\odot$
1	215.1	0.28	233.2	30.29
	$^{+3.7}_{-3.5}$	±0.35	$^{+3.8}_{-3.7}$	±0.22
2	228.8	0.04	242.2	30.41
	$^{+3.6}_{-4.2}$	$^{+0.35}_{-0.17}$	$^{+3.6}_{-4.3}$	±0.21
3	**224.0**	**−2.49**	**239.6**	**30.40**
	$^{\mathbf{+3.9}}_{\mathbf{-3.8}}$	$\mathbf{\pm0.47}$	$^{\mathbf{+4.0}}_{\mathbf{-3.9}}$	$\mathbf{\pm0.20}$
4	224.0	−2.46	239.5	30.40
	±4.0	$^{+0.61}_{-0.63}$	±4.0	±0.20
5	224.0	−2.64	240.2	30.45
	$^{+5.3}_{-4.7}$	$^{+0.83}_{-0.84}$	$^{+2.5}_{-1.9}$	$^{+0.05}_{-0.03}$

Results. XIII

N	DM	L'	R_0 (kpc)	ω_0 $\left(\frac{\text{km/s}}{\text{kpc}}\right)$	A $\left(\frac{\text{km/s}}{\text{kpc}}\right)$	$u_\odot$ $\left(\frac{\text{km}}{\text{s}}\right)$	$v_\odot$ $\left(\frac{\text{km}}{\text{s}}\right)$	$w_\odot$ $\left(\frac{\text{km}}{\text{s}}\right)$	σ_R $\left(\frac{\text{km}}{\text{s}}\right)$	σ_θ $\left(\frac{\text{km}}{\text{s}}\right)$	σ_z $\left(\frac{\text{km}}{\text{s}}\right)$	θ_2 $\left(\frac{\text{km/s}}{\text{kpc}^2}\right)$	θ_3 $\left(\frac{\text{km/s}}{\text{kpc}^3}\right)$
210	3D	—	8.317	28.43	14.82	3.47	16.41	8.27	20.36	15.79	4.80	−1.83	1.16
			$^{+0.140}_{-0.126}$	±0.39	±0.41	±1.71	$^{+1.92}_{-1.91}$	±0.57	$^{+1.49}_{-1.23}$	$^{+1.49}_{-1.38}$	$^{+0.66}_{-0.64}$	±0.32	±0.20
210	4D	—	7.935	28.3	15.77	6.21	16.0	8.36	11.06	4.8	4.10	−1.29	1.30
			$^{+0.123}_{-0.120}$	±0.2	$^{+0.26}_{-0.25}$	$^{+1.04}_{-1.07}$	±1.0	±0.54	$^{+0.73}_{-0.83}$	±0.9	$^{+0.65}_{-0.64}$	$^{+0.22}_{-0.23}$	$^{+0.18}_{-0.17}$
201	4D	3	7.897	28.46	15.56	6.43	15.67	8.32	**7.13**	**4.64**	**3.45**	−1.30	1.09
			$^{+0.116}_{-0.113}$	±0.22	±0.22	±0.85	$^{+0.93}_{-0.94}$	$^{+0.52}_{-0.53}$	$^{+0.83}_{-0.77}$	$^{+0.84}_{-0.85}$	$^{+0.64}_{-0.65}$	$^{+0.20}_{-0.21}$	$^{+0.14}_{-0.13}$
197	4D	1	**7.881**	**28.43**	**15.46**	**6.09**	**15.55**	**8.22**	(7.13)	(4.64)	(3.45)	**−1.34**	**1.03**
			$^{+0.119}_{-0.115}$	±0.22	±0.23	±0.86	±0.92	±0.52				±0.20	±0.14
197	3D	—	8.370	28.34	14.63	2.90	16.83	8.05	(17.54)	(14.95)	(3.85)	−1.76	1.07
			$^{+0.130}_{-0.122}$	±0.36	±0.40	±1.57	±1.80	±0.54				±0.31	±0.20

The second column "DM" indicates the dimension of the method: "3D" means that catalog values of parallaxes were used (parallax errors were not taken into account); "4D" means that the reduced parallaxes were found (parallax errors were taken into account).

Results. XIV

$$\sigma_0 = 0.804 \pm 0.041.$$

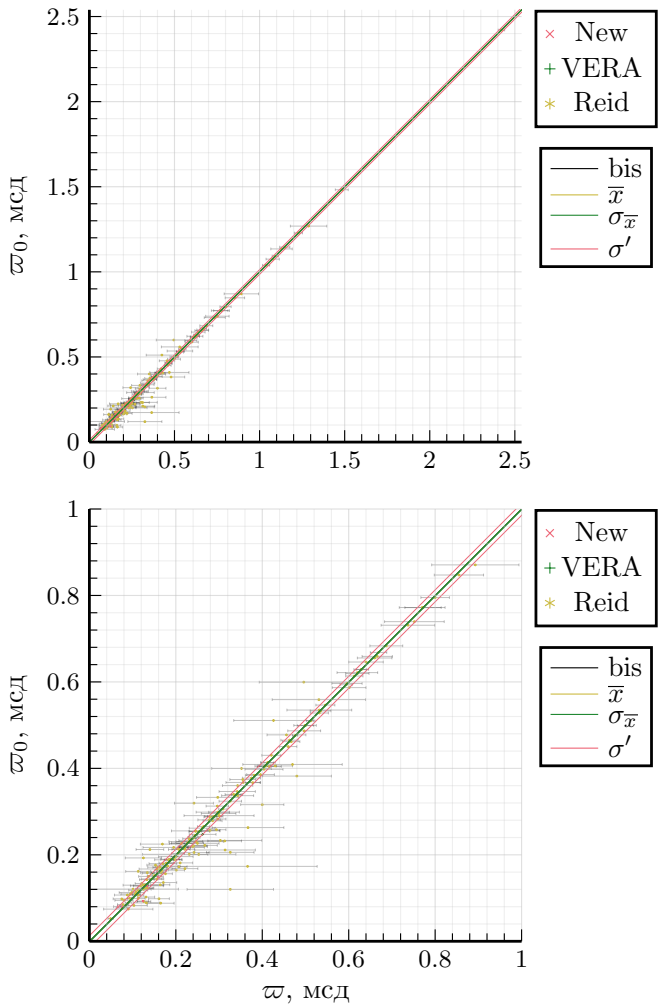

Рис. 11. Соотношение исходных и приведенных параллаксов (выборка HMSFRs, $n_o = 3$). Биссектриса (прямая $y = x$) — линия серого цвета, набор отстоящих от неё по вертикали линий: средняя систематическая ошибка параллаксов $\overline{x} = \Delta\varpi$ (желтая линия, линия модели зависимости) и её ошибка $\sigma_{\overline{x}}$ (зеленые линии, показывающие доверительную область модели), а также взвешенный стандарт выборки σ' (красные линии, показывающие средний разброс). Биссектриса сливается с линией модели зависимости, поскольку величина $\Delta\varpi$ близка к нулю.

Results. XV

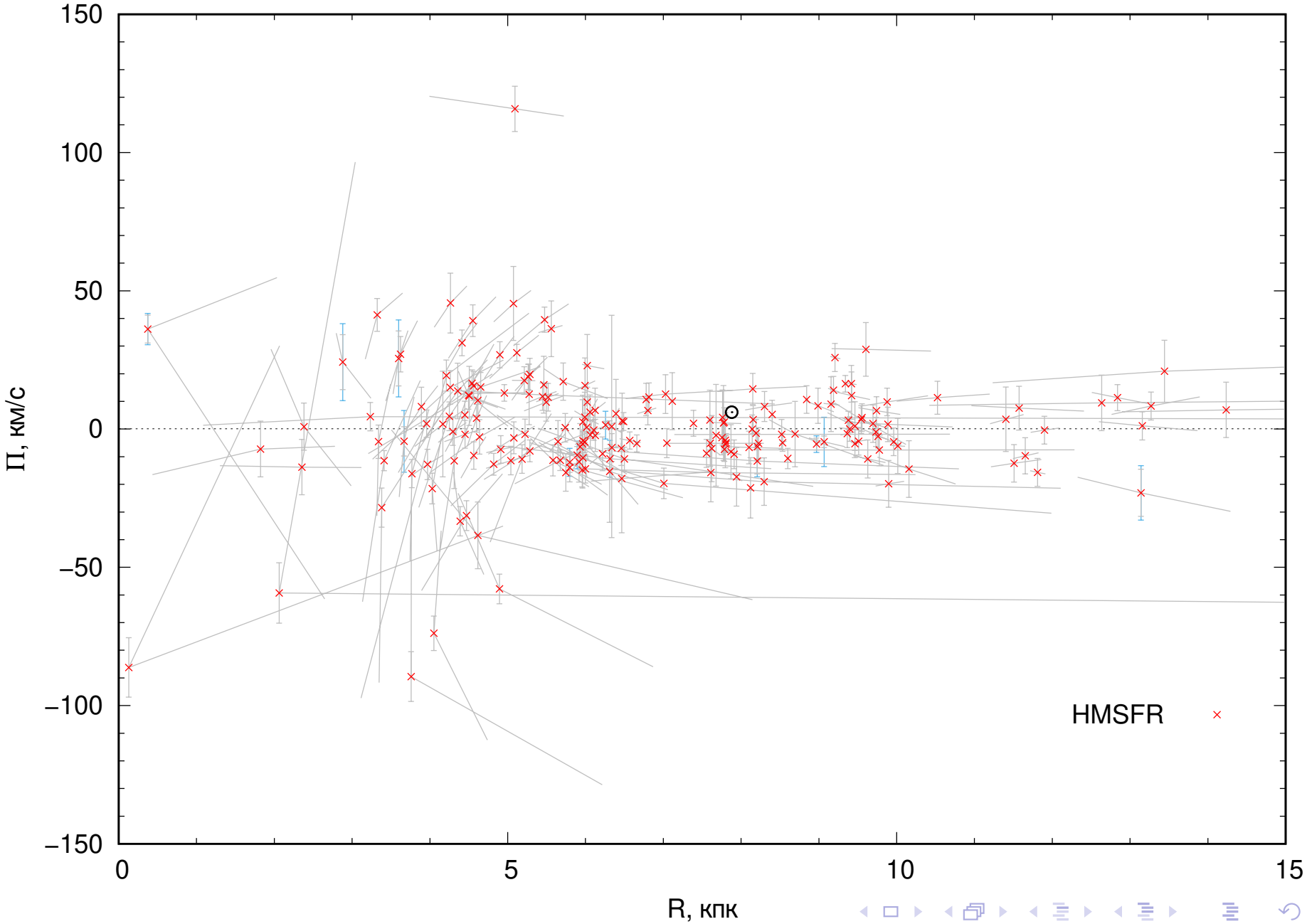

Conclusions. I

1. An algorithm for spatial-kinematic modeling of a homogeneous planar subsystem of Galaxy objects in a three-dimensional velocity field has been developed and implemented, taking into account random errors of heliocentric distances.
2. It is shown that the omission of random parallax errors leads to significant biases for parameters, in particular, to an underestimation of the distance from the Sun to the center of the Galaxy R_0 by $\sim$0.4–0.5 kpc.
3. An estimate of $R_0 = 7.88 \pm 0.12$ kpc (HMSFRs sample, $N = 197$, $n_o = 3$) is derived, which is currently the most statistically and systematically accurate of the estimates obtained from maser sources.
4. It is shown that the uncertainties of maser parallaxes indicated in the catalogs are overestimated by about $1/5$.

Supplement

Актуальные задачи.

- Дальнейшее совершенствование метода.
- Пополнение базы данных о мазерных источниках и изучение их подсистем в Галактике.
- Применение к другим типам опорных объектов (цефеиды и др.).
- Кинематическая калибровка фотометрических шкал расстояний и исправление систематических ошибок измерений параллаксов.
- В перспективе: вклад в решение проблемы природы спиральной структуры Галактики.
- ...